

Closed-Loop Input Shaping with Smith Predictor and Quantitative Feedback Control

Withit Chatlatanagulchai^{1,*} and Puwadon Poedaeng¹

¹ Control of Robot and Vibration Laboratory, Department of Mechanical Engineering, Faculty of Engineering, Kasetsart University, 50 Phahonyothin Rd., Chatuchak, Bangkok, 10900

*Corresponding Author: fengwtc@ku.ac.th, Tel. +66(0) 2797-0999 ext. 1803, 1804, Fax. +66(0) 2579-4576

Abstract

Input shaping is a technique to reduce residual vibration. The technique is based on destructive interference of impulse responses, that is, an impulse response can be cancelled by another impulse response, given appropriate impulse amplitudes and applied times. Placing the input shaper inside the feedback loop in front of the plant offers several advantages including ease of shaper design, elimination of vibration induced by sensor noise, handling of hard nonlinearities, and improving performance of manual control. However, placing the input shaper inside the feedback loop adds time delays to the closed-loop system, which can limit the amount of bandwidth the feedback controller can achieve. Smith predictor can remove the effect of the time delays by feeding back a prediction of the future output to the controller. In this paper, for the first time, the Smith predictor is applied to an input-shaped flexible plant, having Quantitative feedback control as feedback control system. The simulation results show that the performance of the closed-loop control is improved significantly for an input-shaped flexible plant.

Keywords: Input shaping; Vibration reduction; Quantitative feedback control; Smith predictor.

1. Introduction

Input shaping is a technique to reduce residual vibration. The technique is based on destructive interference of impulse responses, that is, an impulse response can be cancelled by another impulse response, given appropriate impulse amplitudes and applied times.

The input shaper is frequently placed inside the feedback loop for advantages such as ease of shaper design, elimination of vibration induced by sensor noise, handling of hard nonlinearities, and improving performance of manual control.

However, two important disadvantages are that the input shaper inside the feedback loop cannot suppress vibration induced by disturbances and that the time delay in the input shaper can seriously limit the performance of the feedback controller.

In this paper, for the first time, Smith predictor is placed inside of the loop together with quantitative feedback control. Under perfect model assumption, Smith predictor removes the effect of the time delay from the feedback loop, allowing the feedback controller to be designed

DRC-22

without limit from time delay. The quantitative feedback control can be designed to meet frequency-domain disturbance rejection specification. As a result, the proposed system can also reject vibration induced by the disturbances.

The proposed system improves the disadvantages of the closed-loop input shaping whereas still maintains its advantages.

Simulation on a two-mass rigid-flexible system is used to confirm the effectiveness of the proposed system. This simulated system represents majority of the rigid-flexible systems in practice.

The paper is organized in this way. Section 2 shows details of the two-mass rigid-flexible system including its equations of motion, state-space model, and transfer functions and provides an example of impulse response, which shows its flexible behavior. Section 3 discusses advantages and disadvantages of closed-loop input shaping system and introduces the ZV input shaper. Section 4 presents the proposed closed-loop input shaping system with Smith predictor and quantitative feedback control. The section contains details on Smith predictor and simulation results by applying the proposed system to the rigid-flexible system. Conclusions are given in Section 5.

2. Two-Mass Rigid-Flexible System

Consider a two-mass rigid-flexible system in Fig. 1. In general, the system represents two entities, connected via a flexible part, which encompasses a large majority of actual rigid-flexible systems. The driving one has an absolute

position and mass of x_0 and m_0 , and the driven one has x_1 and m_1 . k , c_0 , and c are spring stiffness and two damping constants. f is the control force. The objective is to move both masses from the origin to a displacement X with zero residual vibrations and in a shortest time possible T , that is,

$$\begin{Bmatrix} x_0 \\ x_1 \end{Bmatrix} \Big|_{t=T} = \begin{Bmatrix} X \\ X \end{Bmatrix}, \quad \begin{Bmatrix} \dot{x}_0 \\ \dot{x}_1 \end{Bmatrix} \Big|_{t=T} = \begin{Bmatrix} 0 \\ 0 \end{Bmatrix}.$$

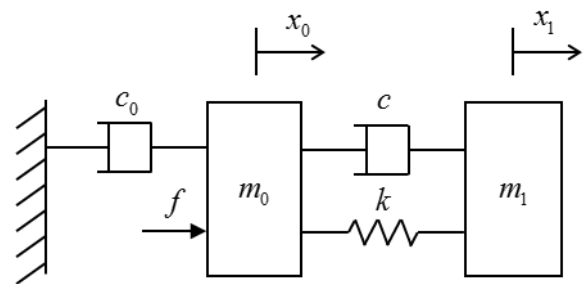


Fig. 1 Two-mass rigid-flexible system.

The equations of motion of the system in Fig. 1 can be found as

$$\begin{aligned} m_0 \ddot{x}_0 + c(\dot{x}_0 - \dot{x}_1) + k(x_0 - x_1) + c_0 \dot{x}_0 &= f, \\ m_1 \ddot{x}_1 - c(\dot{x}_0 - \dot{x}_1) - k(x_0 - x_1) &= 0. \end{aligned}$$

The corresponding state-space model with output x_1 is given by

$$\begin{Bmatrix} \dot{x}_0 \\ \ddot{x}_0 \\ \dot{x}_1 \\ \ddot{x}_1 \end{Bmatrix} = \begin{bmatrix} 0 & 1 & 0 & 0 \\ -\frac{k}{m_0} & -\frac{(c+c_0)}{m_0} & \frac{k}{m_0} & \frac{c}{m_0} \\ 0 & 0 & 0 & 1 \\ \frac{k}{m_1} & \frac{c}{m_1} & -\frac{k}{m_1} & -\frac{c}{m_1} \end{bmatrix} \begin{Bmatrix} x_0 \\ \dot{x}_0 \\ x_1 \\ \dot{x}_1 \end{Bmatrix} + \begin{Bmatrix} 0 \\ \frac{1}{m_0} \\ 0 \\ 0 \end{Bmatrix} f, \quad y = [0 \ 0 \ 1 \ 0]x.$$

DRC-22

The corresponding transfer function from x_0 to x_1 is given by

$$P_2(s) = \frac{X_1(s)}{X_0(s)} = \frac{cs + k}{m_1s^2 + cs + k},$$

and from f to x_0 is given by

$$P_1(s) = \frac{X_0(s)}{F(s)} = \frac{m_1s^2 + cs + k}{\left[\begin{array}{l} m_0m_1s^4 + (m_0c + m_1c + m_1c_0)s^3 \\ + (m_0k + m_1k + cc_0)s^2 + c_0ks \end{array} \right]}.$$

Therefore, the transfer function from f to x_1 is given by

$$P(s) = \frac{X_1(s)}{F(s)} = \frac{cs + k}{\left[\begin{array}{l} m_0m_1s^4 + (m_0c + m_1c + m_1c_0)s^3 \\ + (m_0k + m_1k + cc_0)s^2 + c_0ks \end{array} \right]}. \quad (1)$$

For simulation purpose, let $m_0 = 2$ kg, $m_1 = 3$ kg, $c = 0.1$ kg.s⁻¹, $c_0 = 30$ kg.s⁻¹, and $k = 1$ kg.s⁻². The response x_1 from an impulse input f is shown in Fig. 2, where the effect of the flexible mode, with $\omega_n = 0.58$ rad.s⁻¹ and $\zeta = 5.8 \times 10^{-2}$, is evident.

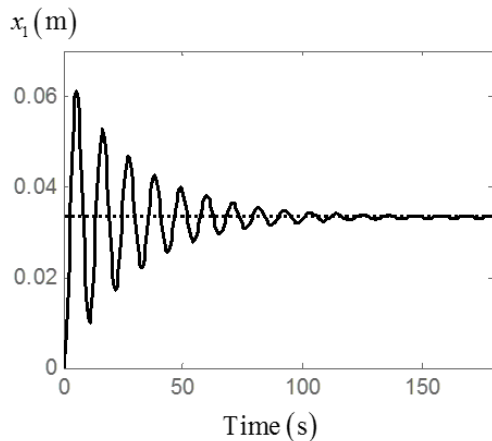


Fig. 2 Impulse response of the two-mass rigid-flexible system.

3. Closed-Loop Input Shaping

3.1 Closed-loop input shaping system

Consider the system in Fig. 3. G is the feedback controller. F is the prefilter. G and F will be designed from the quantitative feedback theory [2]. IS is the input shaper [3]. For clarity, the simplest ZV input shaper is used in this paper. Its impulse amplitudes are given by

$$A_1 = \frac{1}{1+K}, \quad A_2 = \frac{K}{1+K}, \quad K = e^{-\frac{\zeta\pi}{\sqrt{1-\zeta^2}}}, \quad (2)$$

and its impulse time locations are given by

$$t_1 = 0, \quad t_2 = \frac{\pi}{\omega_n \sqrt{1-\zeta^2}}.$$

It was shown by [4] that the input shaper works by placing its zeros over the flexible poles of the plant. NL represents hard nonlinearities such as deadzone, backlash, saturation, and rate limit. P is the plant. r , y , n , d_i , and d_o represent reference input, plant output, noise, plant-input disturbance, and plant-output disturbance.

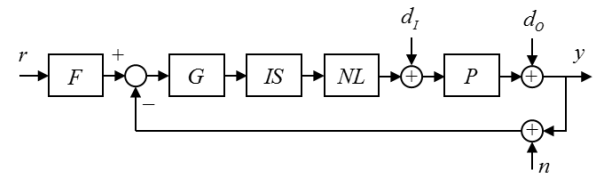


Fig. 3 Closed-loop input shaping.

3.2 Advantages

The advantages of the closed-loop input shaping system in Fig. 3 are as follows:

- 1) According to [5], human control of flexible systems can be improved using the closed-loop input shaping system because the input shaper, placed in front of the flexible plant, can effectively remove the flexibility from the plant.
- 2) When plant has hard nonlinearities, performance of input shaping is degraded.

DRC-22

Closed-loop input shaping allows effective remedy for this degradation because the input shaper is placed directly in front of the plant, so it can be relatively easy to adjust [6].

3) The input shaper in the closed-loop input shaping system can suppress vibration induced by reference and noise [7]. Consider the relationship

$$\left| \frac{Y(s)}{N(s)} \right| = \left| \frac{Y(s)}{R(s)} \right| = \left| \frac{P_n(s)IS(s)G(s)F(s)}{P_d + P_n(s)IS(s)G(s)} \right|,$$

where the hard nonlinearities NL are neglected for simplicity and P_n and P_d are numerator and denominator of the plant P . The closed-loop system's flexible poles contained in P_d are canceled by the zeros of the input shaper IS in the numerator.

4) It is relatively easy to design the input shaper when it is placed directly in front of the plant as opposed to in front of a closed-loop system.

3.3 Disadvantages

1) The input shaper in the closed-loop input shaping system cannot suppress vibration induced by disturbances [7]. Consider two relationships

$$\left| \frac{Y(s)}{D_o(s)} \right| = \left| \frac{P_d(s)}{P_d(s) + P_n(s)IS(s)G(s)} \right|,$$

$$\left| \frac{Y(s)}{D_l(s)} \right| = \left| \frac{P_n(s)}{P_d(s) + P_n(s)IS(s)G(s)} \right|.$$

The closed-loop system's flexible poles contained in P_d are not canceled by the zeros of the input shaper IS because there is no IS in the numerator.

2) Input shaper such as the ZV input shaper (2) has a transfer function [8]

$$IS(s) = A_1 + A_2 e^{-t_2 s}. \quad (3)$$

When the input shaper is placed in the loop, it adds a time delay of $t_d = t_2$ to the system. The delay term $e^{-t_2 s} \approx 1 - t_2 s$ can also be viewed as unstable or non-minimum-phase zero. According to [9], the time delay causes constraints

$$\left\| \frac{Y(s)}{D_o(s)} \right\|_{\infty} = \|S\|_{\infty} \geq 1,$$

$$\left\| \frac{Y(s)}{D_l(s)} \right\|_{\infty} = \|SP\|_{\infty} \geq |P(s)|_{s=1/t_2},$$

$$\left\| \frac{Y(s)}{N(s)} \right\|_{\infty} = \left\| \frac{Y(s)}{R(s)} \right\|_{\infty} = \|T\|_{\infty} \geq 1,$$

$$\omega_B < 1/t_2,$$

where S is the sensitivity function, T is the complementary sensitivity function, and ω_B is the system bandwidth. The constraints limit the performance of the closed-loop system. Besides, the unstable zero also leads to instability when using high feedback gain since, as feedback gain increases toward infinity, the closed-loop poles move to the open-loop zeros.

4. Closed-Loop Input Shaping with Smith Predictor

4.1 Smith predictor

According to [10], a closed-loop system with Smith predictor is shown in Fig. 4, where $P = P_0 e^{-\theta s}$ is the plant with time delay θ , P_0 is the plant P without time delay, G is the controller, \hat{P} is the model of P , and \hat{P}_0 is the model of P_0 .

DRC-22

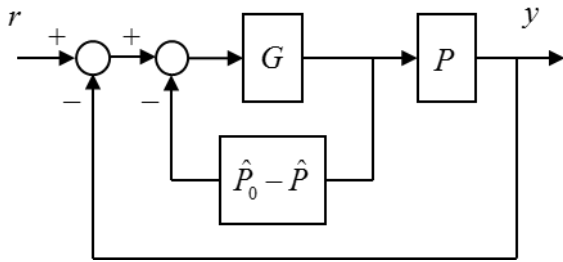


Fig. 4 Closed-loop system with Smith predictor.

Assuming perfect models, that is, $\hat{P} = P$ and $\hat{P}_0 = P_0$, the Smith predictor $\hat{P}_0 - \hat{P}$ results in a transfer function

$$\frac{Y(s)}{R(s)} = \frac{GP}{1 + GP_0},$$

which is equivalent to Fig. 5 where the time delay has been moved out of the loop and from the characteristic equation.

Note that when the models are not perfect, the time delay is not totally removed from the loop. However, there will be less detrimental effect from the time delay.

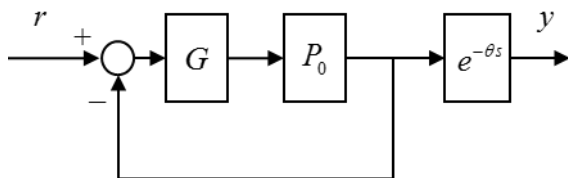


Fig. 5 Equivalent closed-loop system.

4.2 Closed-loop input shaping with Smith predictor

By modifying the system in Fig. 4 and following [11], the closed-loop input shaping with Smith predictor and quantitative feedback control is shown in Fig. 6. In our case, P is the plant (1) without time delay, \hat{P} is its model, and IS is the ZV input shaper (3) with known time delay.

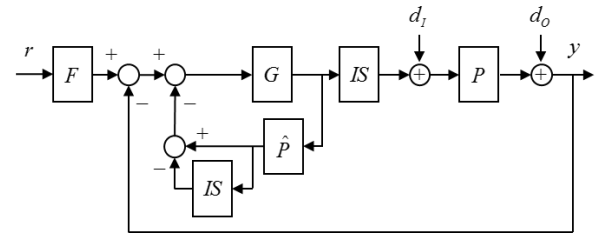


Fig. 6 Closed-loop input shaping system with Smith predictor and quantitative feedback control.

Assuming perfect model $\hat{P} = P$, the Smith predictor $\hat{P} - IS \cdot \hat{P}$ results in a transfer function

$$\frac{Y(s)}{R(s)} = \frac{P(s)IS(s)G(s)F(s)}{1 + G(s)\hat{P}(s)},$$

which is equivalent to Fig. 7 where the ZV input shaper has been moved out of the loop and from the characteristic equation.

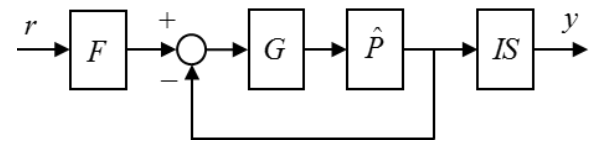


Fig. 7 Equivalent closed-loop system.

Therefore, the quantitative feedback control can be designed from the plant model \hat{P} without the time delay. After G and F are obtained, they can be implemented with the Smith predictor as in Fig. 6.

4.3 Simulation results

Consider the flexible plant (1). This section shows design of the proposed system that improves the disadvantages in Section 3.3.

Assume that the two damping constants have $\pm 10\%$ uncertainties, that is, $c_0 \in \{0.09, 0.11\}$ and $c \in \{27, 33\}$.

The quantitative feedback control [2] ensures the following frequency-domain specifications:

DRC-22

$$\left| \frac{PG}{1+PG} \right| < 3 \text{ dB}, \quad (4)$$

$$\alpha \leq \left| \frac{PGF}{1+PG} \right| \leq \beta, \quad (5)$$

$$\left| \frac{1}{1+PG} \right| < -3 \text{ dB}, \quad (6)$$

will be met for frequencies $\omega \in \{0.05, 0.1, 0.2, 0.5, 0.8, 1, 3, 7, 11\}$ rad/s, which are around the bandwidth of the nominal plant (1), and for all plant uncertainties. α and β are chosen as those in Table 1.

Table. 1 Bounds for tracking specification.

$\omega \times 10^{-1}$ (rad/s)	0.5	1	2	5	8	10
β (dB)	0	0	0	-0.3	-1.5	-3
α (dB)	-0.6	-0.6	-0.8	-1.6	-4	-6

Note that (4) is the stability margin specification that implies gain margin > 4.65 dB and phase margin > 41.46 degrees, (5) is the tracking specification, and (6) is the plant-output disturbance rejection specification.

The controller G was found from loop-shaping to be

$$G = \frac{144.85(s+0.01106)(s+0.6241)}{s}, \quad (7)$$

which consists of an integrator and two real zeros. The final open-loop shape as well as the combined bounds, representing the specifications (4) to (6), are shown in Fig. 8. The open-loop frequency responses $L(j\omega)$ for all frequencies of interest lie in the allowable regions.

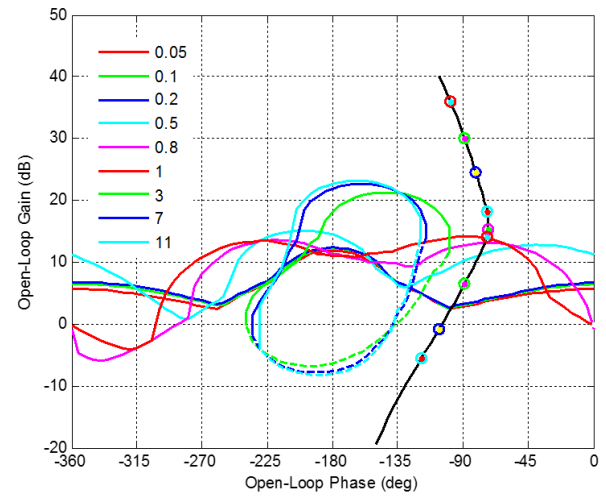


Fig. 8 Bounds on the Nichols chart and final loop shape $L(s) = G(s)P(s)$.

The prefilter F was found from loop-shaping to be

$$F(s) = \frac{0.68132}{s^2 + 1.167s + 0.6813}, \quad (8)$$

which consists of two complex poles.

The frequency-domain specifications (4) to (6) are simulated for 9 plant models spanning the uncertain sets of c_0 and c . The results are shown in Fig. 9, which shows that all specifications are met for all plant uncertainties.

DRC-22

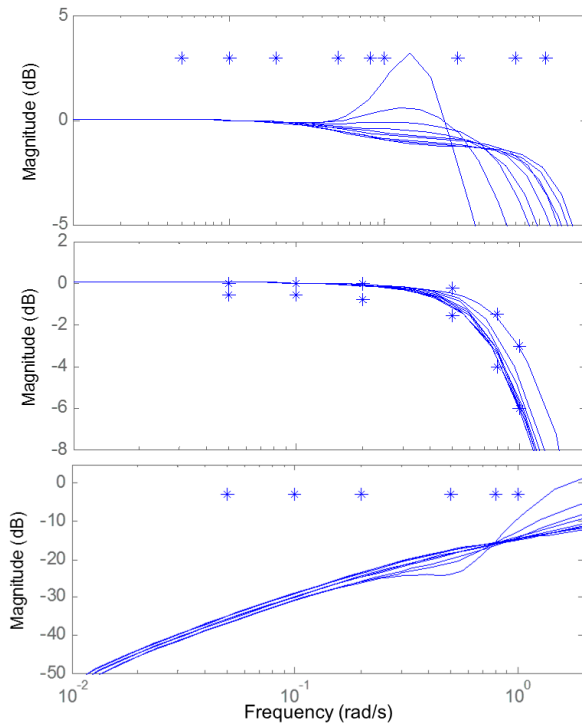


Fig. 9 Simulation results. (Top) $|PG/(1+PG)|$. (Middle) $|PGF/(1+PG)|$. (Bottom) $|1/(1+PG)|$. Asterisks mark corresponding bounds.

The closed-loop system in Fig. 6 is simulated with \hat{P} and P as in (1), G as in (7), F as in (8), and IS as in (3) and (2). The system outputs y when the reference input r is a step function for all 9 plant cases are shown in Fig. 10(Top) and when the plant-output disturbance d_o is a step function are shown in Fig. 10(Bottom). It can be seen that the output tracks the shaped reference really well without oscillation even when the plant is very flexible. The proposed system also results in good plant-output disturbance rejection. Again, oscillation induced by the disturbance is suppressed by the controller.

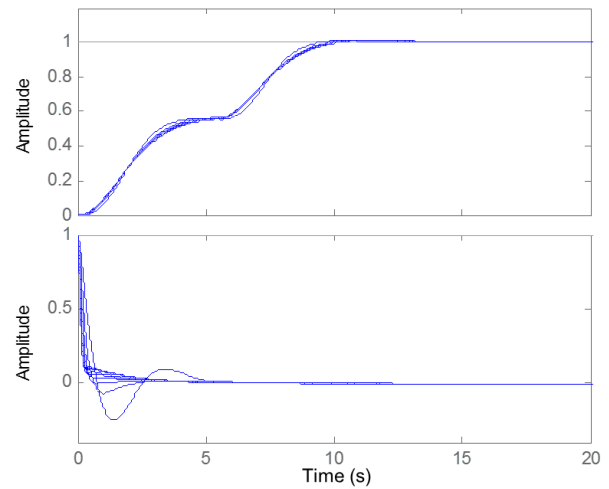


Fig. 10 Simulation results. (Top) System output y to a step reference r . (Bottom) System output y to a step plant-output disturbance d_o .

5. Conclusions

Closed-loop input shaping where the input shaper is placed inside the feedback loop is known to have two disadvantages. First, the input shaper cannot suppress vibration induced by disturbances. Second, the time-delay brought about by the input shaper limits the performance of the feedback controller.

This paper shows that by using Smith predictor. The time delay by the input shaper can be removed from the loop. As a result, the feedback controller's performance is not limited by it. Moreover, by using the quantitative feedback control, disturbance rejection specifications can be imposed resulting in a feedback control system that can suppress vibration induced by the disturbance.

Note that by using the proposed system, the advantages of the closed-loop input shaping listed in Section 3.2 are still attained.

This work assumes perfect model. When the model is not perfect, the influence from the time delay will not be removed totally from the

DRC-22

feedback loop. However, the quantitative feedback control should still be used to assess the achievable performance of the closed-loop system quantitatively. This is the subject of our future work.

6. Acknowledgements

The authors would like to thank Craig Borghesani and Terasoft, Inc for their evaluation copy of the QFT Matlab toolbox.

7. References

- [1] Bhat, S.P. and Miu, D.K. (1990). Precise point-to-point positioning control of flexible structures, *Journal of Dynamic Systems, Measurement, and Control*, vol. 112, pp. 667 – 674.
- [2] Horowitz, I. (1993). *Quantitative Feedback Design Theory*, QFT Publications, Boulder.
- [3] Singer, N.C. and Seering, W.C. (1990). Preshaping command inputs to reduce system vibration, *ASME J. of Dynamics System, Measurement and Control*, vol. 112(1), pp. 76 – 82.
- [4] Singh, T. and Vadali, S.R. (1993). Robust time-delay control, *Journal of Dynamic Systems, Measurement, and Control*, vol. 115, pp. 303 – 306.
- [5] Potter, J.J. and Singhose, W. (2013). Improving manual tracking of systems with oscillatory dynamics, *IEEE Transactions on Human-Machine Systems*, vol. 43(1), pp. 46 – 52.
- [6] Huey, J.R. and Singhose, W. (2010). Trends in the stability properties of CLSS controllers: a root-locus analysis, *IEEE Transactions on Control Systems Technology*, vol. 18(5), pp. 1044 – 1056.
- [7] Huey, J.R., Sorensen, K.L. and Singhose, W.E. (2008). Useful applications of closed-loop signal shaping controllers, *Control Engineering Practice*, vol. 16, pp. 836 – 846.
- [8] Singh, T. and Vadali, S.R. (1993). Robust time-delay control, *Journal of Dynamic Systems, Measurement, and Control*, vol. 115, pp. 303 – 306.
- [9] Skogestad, S. and Postlethwaite, I. (2005). *Multivariable Feedback Control*, John Wiley and Sons, New York.
- [10] Palmor, Z.J. (2011). Time-delay compensation: Smith predictor and its modifications. In Levine, W.S. (Ed.), *The Control Handbook: Control System Fundamentals* (2 ed., pp. 124 – 146), CRC Press, Boca Raton.
- [11] Kucera, V. and Hromcik, M. (2011). Delay-Based Input Shapers in Feedback Interconnections, paper presented in the IFAC World Congress, Milano, Italy.